WAVE SCATTERING BY THE DEFORMED FACET OF A DIELECTRIC SLAB WAVEGUIDE

A. V. Brovko*, A. B. Manenkov**, A. G. Rozhnev*, I. G. Tigelis***

*Saratov State University, ul. Astrakhanskaya 83, Saratov, 410026, Russia
e-mail: brovko@forpost.ru,
**P. Kapitza Institute for Physical Problems, Russian Academy of Sciences,
ul. Kosygina 2, Moscow, 117973, GSP-1, Russia,
***University of Athens, Department of Physics, Applied Physics Division,
Electronics Laboratory, Building V, Panepistimiopolis, Zografou, 157 84 Athens, Greece.

Abstract

The problem of the electromagnetic wave diffraction by a smooth and non-smooth end of a planar dielectric waveguide is examined. The analysis is made by several techniques, including the finite difference time domain method. The guided-mode reflection coefficient as well as the near and far-field distributions are calculated for different deformations of the facet surface.

1. INTRODUCTION

This paper deals with the guided-mode scattering from an ended planar dielectric waveguide with a deformed facet surface. The similar problem of mode scattering from the perfect facet (with plane surface) has been examined in many works [1-6]. At the same time, the study of systems with deformed surface can be a subject of considerable interest, for example, to estimate the influence of this surface defects on the reflectivity. Besides, structures with deformed ends are promising for optical sensor applications.

The stated problem is solved by using the Finite Difference Time Domain (FDTD) method [7-9]. This method is universal and permits to study both the smooth and non-smooth (deformed) geometries. Furthermore, the smooth geometry is also studied by the Integral Equation Method with Accelerated Parameters (IEMAP) and the Variational Technique (VT) [5, 6]. The data obtained by the two last methods are used to check the accuracy of the FDTD method.

In this paper only the TE case is examined. In Section 2 we present a brief description of the method used and in Sections 3-4 we give the results for the smooth and deformed facets.

2. THE METHODS OF THE ANALYSIS

Figure 1 shows the geometries of the problem for the case of the perfect (a) and imperfect (b, c) facet surfaces.

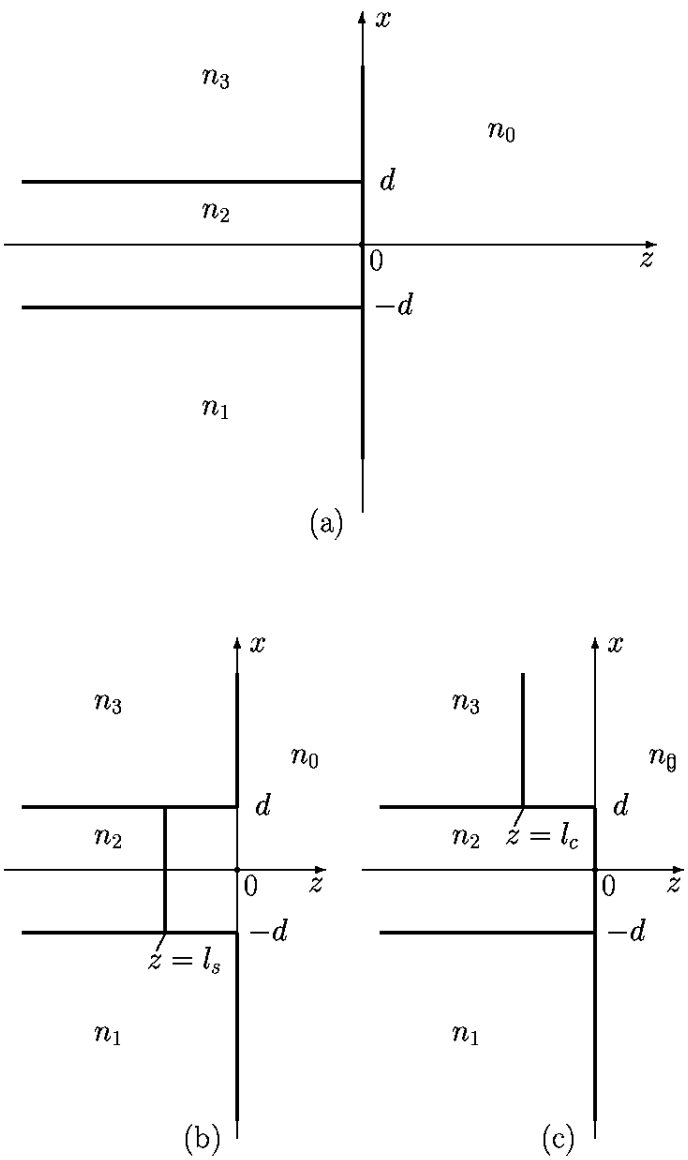

Figure 1. The facet geometries: (a) perfect guide end; (b) the end with the slab shift; (c) the end with the cover shift.

When the FDTD method is applied, the initial problem of monochromatic wave diffraction is replaced by an auxiliary non-stationary one [7-9]. For the system under consideration, we set the initial field distribution at the instant of time $t = 0$ as a wave packet, which is similar to the guided-mode field limited along the coordinate z. Then, we apply the usual FD scheme for the simulation of the packet propagation along the waveguide and its diffraction by the abrupt termination. Finally, the output characteristics of the problem at the specified frequency ω are determined by the Fast Fourier analysis of the FDTD solution. Note that the main advantage of this method is the explicit form of the solution of the algebraic equations.

Below, we briefly describe the basic equations of this method. For the TE case, there are only three nonzero components E_y, H_x and H_z, which obey the following equations:

$$\frac{\partial E_y}{\partial x} = -\mu_v \frac{\partial H_z}{\partial t}, \qquad \frac{\partial E_y}{\partial z} = \mu_v \frac{\partial H_x}{\partial t}, \qquad \frac{\partial H_x}{\partial z} - \frac{\partial H_z}{\partial x} = \frac{\partial D_y}{\partial t}. \tag{1}$$

These equations should be completed by the material equation, i.e.,

$$D_y = \varepsilon E_y, \qquad \varepsilon = n^2(x,z)\varepsilon_v, \tag{2}$$

where ε_v is the permittivity of the vacuum and n is the refractive index.

To discretise the above equations we introduce the rectangular mesh with the coordinate steps Δz and Δx in the plane xOz [9, 10]. The coordinates of the mesh nodes are $(i\Delta z,\ j\Delta x)$, where i and j are integer numbers. We search the values of the electric field in the nodes at the discrete instants of time $t_n = n\Delta t$ (Δt is a time step) and the values of the magnetic field in the nodes of the mesh shifted by a half of the steps $\Delta z/2$ and $\Delta x/2$ at the instants of time $t_{n-1/2} = (n-1/2)\Delta t$. Using the standard approach leads to the algebraic equations for the fields values in the nodes of the mesh [7-10]:

$$D_y^{(n+1)}(i,j) = D_y^{(n)}(i,j) + \frac{\Delta t}{\Delta z}\left[H_x^{(n+1/2)}(i+1/2,j) - H_x^{(n+1/2)}(i-1/2,j)\right]$$

$$-\frac{\Delta t}{\Delta x}\left[H_z^{(n+1/2)}(i,j+1/2) - H_z^{(n+1/2)}(i,j-1/2)\right] \tag{3}$$

$$H_z^{(n+1/2)}(i,j+1/2) = H_z^{(n-1/2)}(i,j+1/2) - \frac{\Delta t}{\mu_v \Delta x}\left[E_y^{(n)}(i,j+1) - E_y^{(n)}(i,j)\right] \tag{4}$$

$$H_x^{(n+1/2)}(i+1/2,j) = H_x^{(n-1/2)}(i+1/2,j) + \frac{\Delta t}{\mu_v \Delta z}\left[E_y^{(n)}(i+1,j) - E_y^{(n)}(i,j)\right] \tag{5}$$

We use the standard denotations [9] for the values of the fields in the node points, i.e., $E_y^{(n)}(i,j) = E_y(i\Delta z, j\Delta x, n\Delta t)$. In the discrete form, equation (2) is written as follows: $E_y^{(n+1)}(i,j) = D_y^{(n+1)}(i,j)/\varepsilon(i,j)$. Note that in these equations the order of the derivative approximations by the finite differences are $O(\Delta z^2)$, $O(\Delta x^2)$ and $O(\Delta t^2)$. The FDTD algorithm converges under the Courant stability condition, which has the form: $c\Delta t < \min[n(x,z)]\Big/\sqrt{(1/\Delta z)^2 + (1/\Delta x)^2}$ (where c is the light velocity). From the

above equations it is seen that the values of the fields at the instants of time t_{n+1} and $t_{n+1/2}$ are derived explicitly from the values of the fields in the previous instants; therefore, these formulas give the explicit solution of the problem.

The waveguide structure under consideration is open and in order to model it we have to describe the far zone fields or to bound the considered domain with eliminating the influence of the boundaries. For this purpose we apply the Perfectly Matched Layers (PML) technique [9-12]. The structure in question is placed into a box with "thick" walls. The parameters of the walls are chosen so that the reflection of the incident wave from the boundary is small, while at the same time the absorption of the wave inside the wall is large. In the walls the fields are computed with the finite difference scheme, which uses the modified equations and the special medium parameters of the walls. These equations and the procedure of the choice of the wall medium parameters are not considered here; the reader can find the details in [10-12]. Note that for the geometry under consideration the results are slightly depend on the parameters of the walls.

The FDTD algorithm gives the time solution $E_y(x,z,t)$, which describes the wave packet diffraction process. Then, applying the Fourier transformation to the solution we can calculate the reflection coefficient at the specified frequency ω. The electric field $E = E_y(x,z,t)$ in the waveguide part of the domain ($z<0$) can be expressed as a Fourier integral of the waveguide eigenmodes expansion [13-15]:

$$E(x,z,t) = \int_{-\infty}^{\infty} \left[\sum_{\alpha=\pm} C_0^{(\alpha)}(\omega) E_0^{(\alpha)}(x,\omega) \exp\left[i(\alpha\beta_0(\omega)z - \omega t) \right] + E_R(x,z,\omega) \right] d\omega \qquad (6)$$

where $E_0^{(+)}$ and $E_0^{(-)}$ denote the complex amplitude of the forward and backward guided mode, respectively, $\beta_0(\omega)$ is the propagation constant of the forward mode, $C_0^{(+)}$ and $C_0^{(-)}$ are the decomposition coefficients, $E_R(x,z,\omega)$ is the complex amplitude of the radiation field. For the dielectric waveguide with the constant profile of the refractive index the guided modes can be calculated with the analytical expressions given in [15, 16]. The complex amplitudes E_R can be written as the integrals of the fields of the continuous spectrum modes. Using the orthogonality relations [13-15] of the waveguide eigenmodes and calculating the inverse Fourier transformation, we derive the expression of the guided modes amplitudes:

$$C_0^{(\alpha)}(\omega)\exp\left[i\alpha\beta_0(\omega)z\right]=\int_{-\infty}^{\infty}\int_{-\infty}^{\infty}[\beta_0(\omega)E_y(x,z,t)/(k\zeta_v)-aH_x(x,z,t)]$$

$$\times\exp(i\omega t)dt\ E_{0y}(x,\omega)dx\ /\ N_0\,, \qquad (7)$$

where N_0 is the norm of the guided mode [13], $\zeta_v=\sqrt{\mu_v/\varepsilon_v}$ is the impedance of the free space, $k=\omega/c$ is the free-space wave number; and the auxiliary parameter α labels the forward and backward modes ($\alpha=\pm$). From equation (7) we derive the formula for the reflection coefficient of the guided mode at the termination plane ($z=0$) at the frequency ω:

$$R(\omega)=C_0^{(-)}(\omega)\big/C_0^{(+)}(\omega)\,. \qquad (8)$$

The above procedure permits to separate the radiation waves and the guided modes from the solution $E_y(x,z,t)$. The other characteristics of the problem could be found in a similar manner.

The smooth geometry of the problem (with planar termination surface) can be also examined by the IEMAP and approximate VT (see above). Note that these approaches are only applicable to the analysis of the monochromatic wave diffraction processes. For the structure under examination the unknown electric field $E=E_y(x,0)$ on the terminal plane $z=0$ (Fig. 1) obeys the integral equation, which can be written in the following symbolic form [5,6]:

$$\hat{\Xi}_e E=E_0 \qquad (9)$$

where $\hat{\Xi}_e$ is an integral operator and $E_0=E_{y0}(x,0)$ is the electric field of the dominant incident guided mode; the time dependence $\exp(-i\omega t)$ is omitted in all equations. In order to solve equation (9) we employ an improved iteration technique, which is a variant of the semi-inversion approach [6]. According to this approach, the integral operator $\hat{\Xi}_e$ of (9) is divided into "dominant" and "small" parts, $\hat{\Xi}_e=\hat{K}_d+\hat{K}_s$. Then, the dominant part of the operator $\hat{K}_d$, which has a simple form, is inversed and the new equation transformed (containing small operator) is solved by the iteration technique. The solution obtained has the form of the Neumann series [5, 6]. With the help of the auxiliary parameters, which are introduced into operators, the norm of the small operator $\hat{K}_s$ can be decreased to accelerate the iteration convergency. The tests have demonstrated that several first iterations give precise results for the problem in question

[6]. It also permits to apply this method to a wide class of discontinuity problems, including strongly asymmetrical systems, where the weak guidance condition is invalid. The variational solution of the problem is also derived from (9). The details of this technique are described in [5, 6] and they are not discussed here.

3. THE SMOOTH GEOMETRIES

At first, we consider the smooth system, where the termination at $z = 0$ is a planar surface (see Fig. 1a). We assume that the refractive index of the dielectric slab ($|x| < d$) is n_2, while the refractive indices of the substrate ($x < -d$) and cover ($x > d$) are n_1 and n_3, respectively, with $n_3 \le n_1 < n_2$. In all the examples considered below we suppose that the free-space wavelength $\lambda = 0.86\,\mu$m, the refractive index of the slab is $n_2 = 3.6$ and the index of the right semi-space ($z > 0$) is $n_0 = 1$. The dominant guided-mode TE_0 is assumed to propagate from $z = -\infty$ to the terminal plane $z = 0$.

In Fig. 2 we present the dependency of the reflected power $|R|^2$ on the slab thickness $2d$. The other problem parameters are $n_1 = n_3 = 3.24$ (symmetrical waveguide). The solid curve is constructed by the FDTD method, the squares by the IEMAP and the dashed line by the VT. To calculate the data presented above, we used a box with sizes 4 μm and 1.5 μm along the coordinate axes Oz and Ox, respectively, and the waveguide portion length was 1.4 μm. The sizes of the square mesh were $\Delta x = \Delta z = 0.01$ μm and the time step was $\Delta t = 0.667 \cdot 10^{-17}$ s. The reflection of the partial rays from the wall box was of the order of $4 \cdot 10^{-4}$.

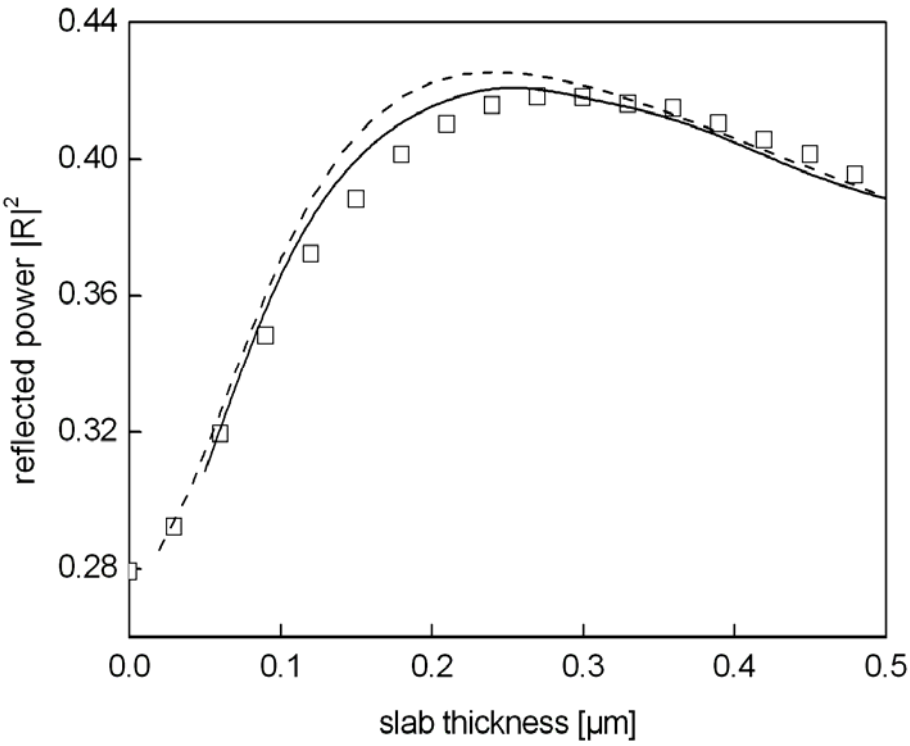

Figure 2. The reflected power versus the slab thickness for the symmetrical waveguide system.

In Fig. 3 we show the far-zone pattern for the problem in question. All the refractive indices are the same as for Fig. 2 and the slab thickness is $2d = 0.25\,\mu$m. The solid curve is constructed by the FDTD method and the squares correspond to the data calculated by the IEMAP. The sense of the dashed line will be explained below. Note that the far-zone pattern was computed with a larger vertical box size ($3 \div 4$ μm).

Fig. 4 shows the dependency $|R|^2$ on the slab thickness $2d$ for the strongly asymmetrical system with $n_1 = 3.24$ and $n_3 = 1.0$. The dominant guided mode of the asymmetrical waveguide has a cutoff; therefore the curve starts from the point with value $2d = 2d_c > 0$, where the reflection coefficient is $R_0 = (n_1 - n_0)/(n_1 + n_0)$. In this figure $|R|^2$ is calculated by the FDTD method (solid curve), IEMAP (squares) and VT (dashed line).

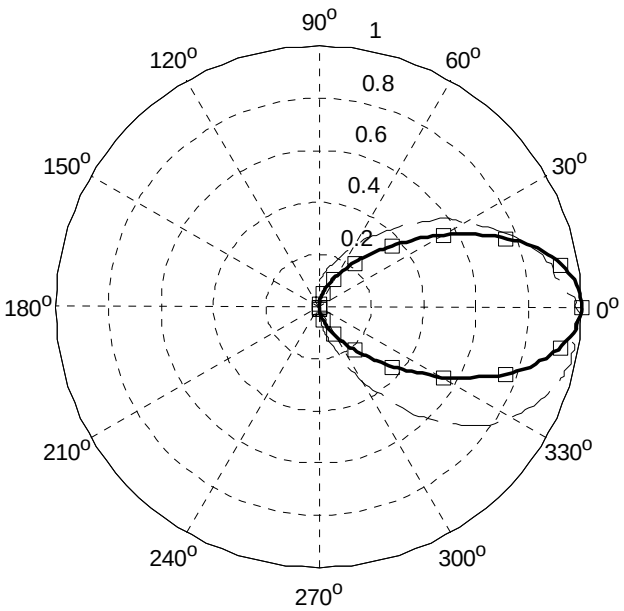

Figure 3. The far-zone pattern for the smooth facet (the solid curve and squares) and for the facet with the cover shift (l_c=-0.5 μm, the dashed line).

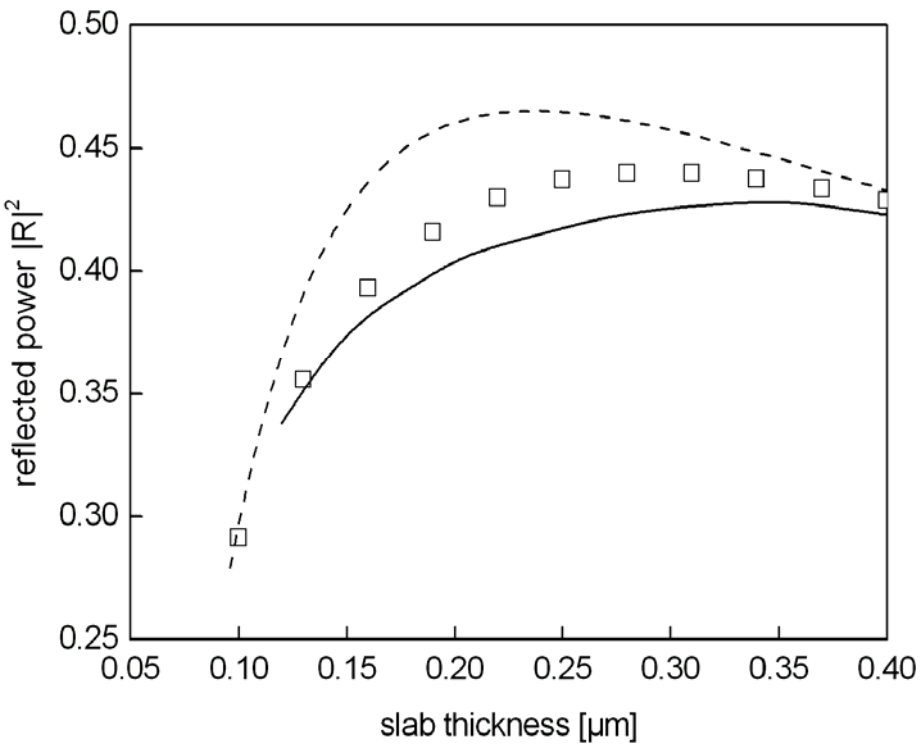

Figure 4. This figure is similar to Fig. 2, but it constructed for the strongly asymmetrical waveguide.

In all these cases the results obtained by the FDTD and IEMAP are in a good agreement. On the other hand, the data calculated by the approximate VT agree well with the results mentioned above, only if the WGC is valid (see Fig. 2). For the strongly

asymmetrical systems (Fig. 4) there is a small difference between the data computed by the VT and the other two methods. The difference is explained by the effect of the wave diffraction by the upper dielectric corner, which is not taken into account with the version of the VT used here.

4. THE DEFORMED (NON-SMOOTH) GEOMETRIES

Next we consider systems with perturbed facet surfaces. The examples of such systems are given in Figs. 1b and 1c. First, we examine the waveguide end where the right slab boundary is shifted (Fig. 1b). Fig. 5 presents the reflected power $|R|^2$ as a function of the coordinate $z = l_s$ of this boundary. The indices of the media are $n_1 = n_3 = 3.24$. The data are calculated by the FDTD method only. The change of $|R|^2$ is explained by the interference of the waves excited by the two discontinuities appeared at the slab waveguide termination surface.

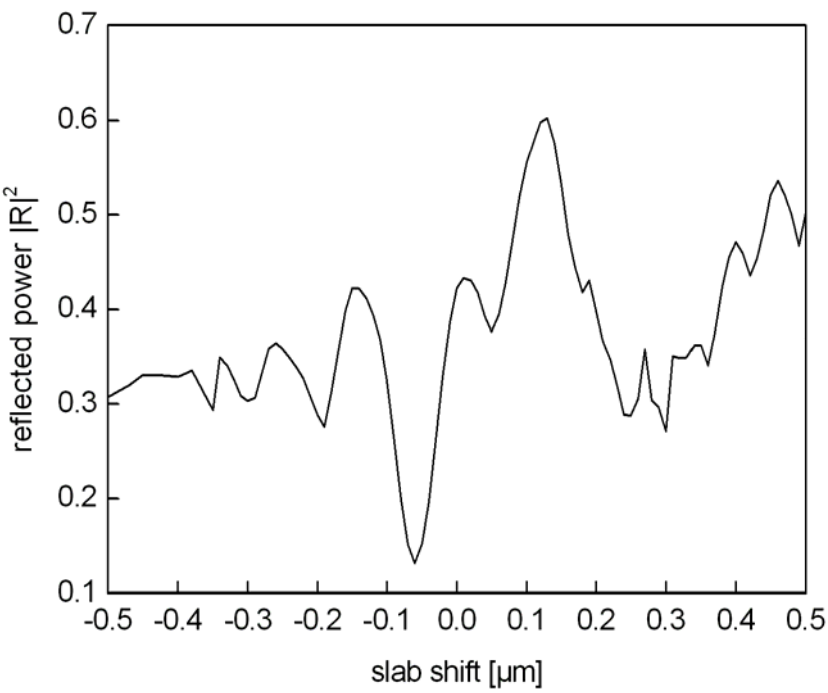

Figure 5. The reflected power versus the coordinate l_s of the shifted slab.

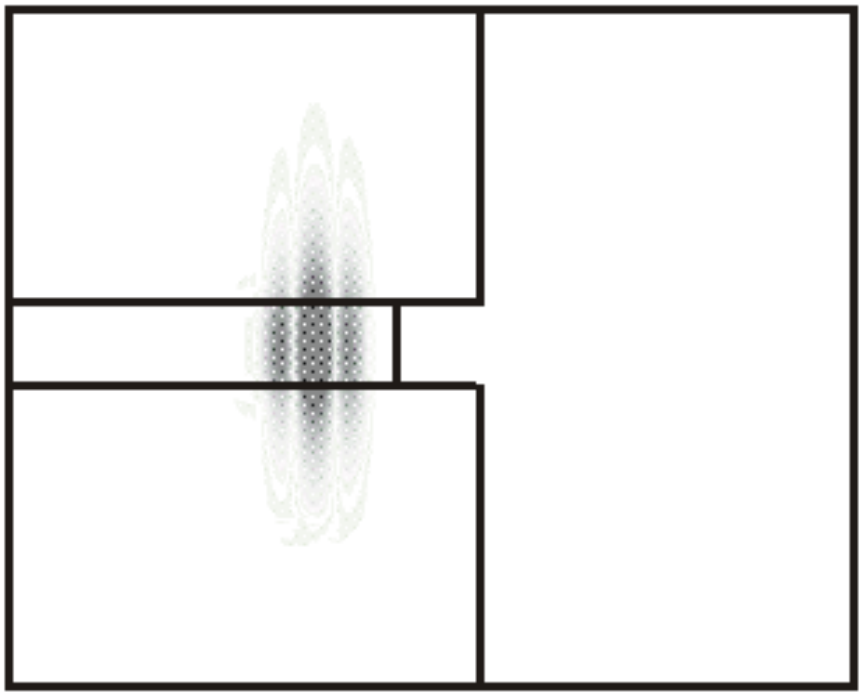

(a)

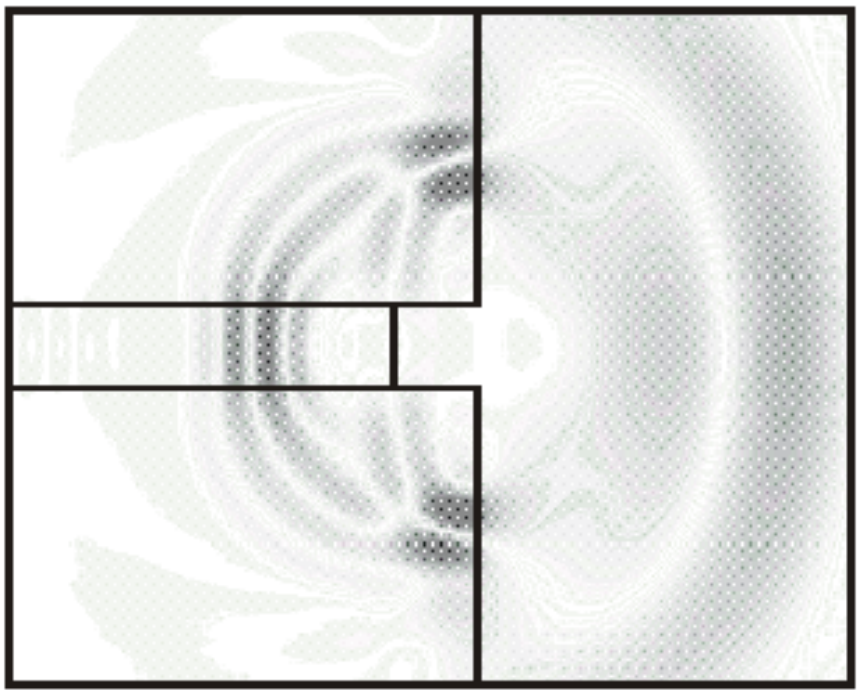

(b)

Figure 6. The field distributions for the system with the slab shift at $t = n\Delta t$: (a) $n = 310$ and (b) $n = 740$.

Fig. 6 shows the field distributions $|E_y(x,z,t)|$ at two instants of time $t_n = n \cdot \Delta t$, with $\Delta t = 2 \cdot 10^{-17}$ s, $n = 310$ for the upper picture (Fig. 6a) and $n = 740$ for the lower picture (Fig. 6b). The shifted slab coordinate is $l_s = -0.25\,\mu$m and other parameters are the same as for Fig. 4. The degree of the black points is proportional to the module of the field magnitude $|E_y(x,z,t)|$. For the system under consideration the radiation to the substrate and to the cover is seen to be sufficiently large.

In Fig. 7 we present the variation of $|R|^2$ with the coordinate $z = l_c$ of the shifted cover. The geometry of the system is shown in Fig. 1c. The problem parameters are the same as for Fig. 2. In this case the mode reflection is also changed due to the interference of the waves excited by the discontinuity appeared at the termination plane. The far-zone pattern for the problem with the cover shift is plotted in Fig. 3 (dashed line). In this case the cover coordinate is $l_c = -0.5$ μm. This perturbation of the waveguide end surface is seen to rotate the pattern (compare all the curves in this figure).

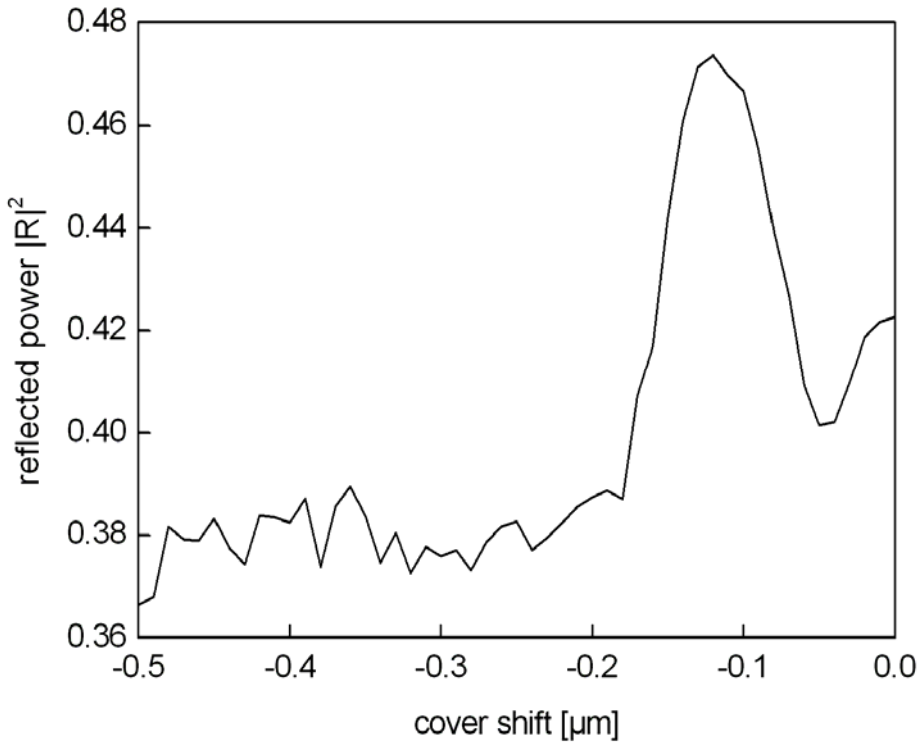

Figure 7. The reflected power versus the coordinate l_c of the shifted cover.

Finally, we consider the facet deformation of the strongly asymmetrical waveguide structure. Fig. 8 presents the dependency $|R|^2$ on the slab shift l_s for such a system

with indices $n_1 = 3.24$ and $n_3 = 1.0$ (the guide without the cover). The other parameters are the same, as for Fig. 4.

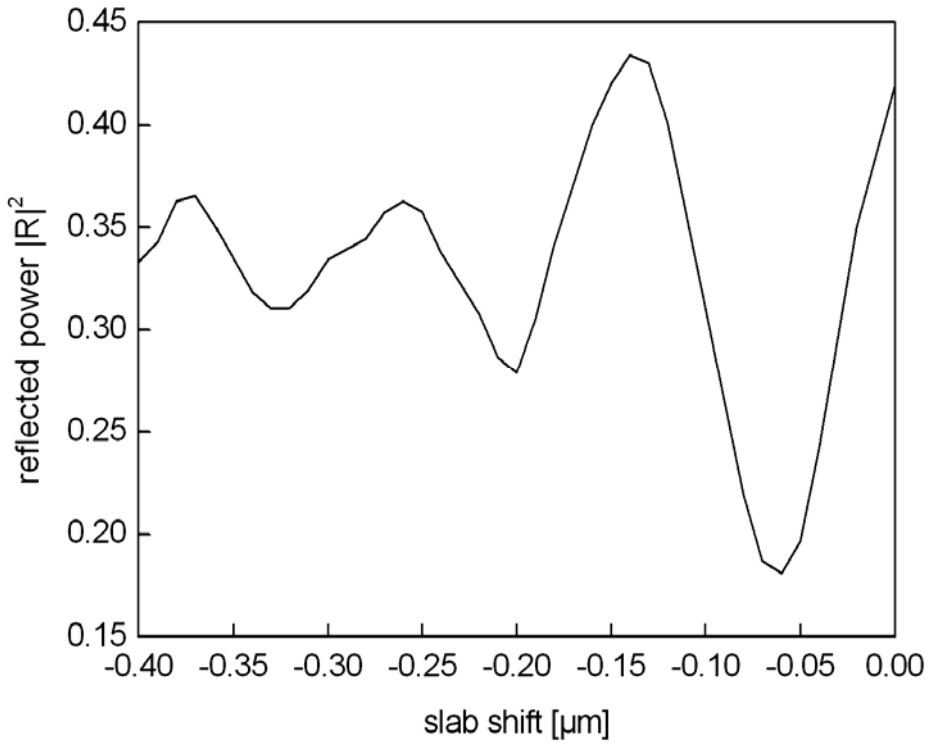

Figure 8. The power reflection coefficient versus the coordinate l_s of the shifted slab for the strongly asymmetrical system.

5. CONCLUSION

We study the influence of the facet deformation of the planar dielectric waveguide end on the scattering characteristics. The numerical simulations have demonstrated that the facet deformations change both the guided-mode reflection coefficient and the field distributions. In particular, the shift of the slab or cover surface radically affects the near zone field distributions, giving the enhanced broadside radiation (to the substrate and cover) and rotates the far-zone pattern. All the effects are explained by the interference of the waves excited by the discontinuities appeared at the termination plane. Such effects seem to be useful for many applications including the design of optical sensors or elements of integrated optics.

ACKNOWLEDGEMENTS

The authors thank the RFBR (grants 00–02–17500 and 02–02–06471) for the partial support of this work. We also thank Prof. N. Uzunoglu for his interest in this work.

REFERENCES

[1] T. Ikegami, “Reflectivity of mode at facet and oscillation mode in double-heterostructure injection lasers”, *IEEE J. Quantum Electron*., vol. 8, no. 6, pp. 470-476, 1972.

[2] T. E. Rozzi, and G. H. In't Veld, “Variational treatment of the diffraction at the facet of d.h. lasers and of dielectric millimeter wave antennas”, *IEEE Trans. Microwave Theory Tech.*, vol. 28, pp. 61-73, Feb. 1980.

[3] C. Vassallo, “Reflectivity of multi-dielectric coatings deposited on the end facet of a weakly guiding dielectric slab waveguide”, *J. Opt. Soc. Am.*, vol. A-5, no. 11, pp. 1918-1928, 1988.

[4] P. C. Kendall, D. A. Roberts, P. N. Robson, et al., “Semiconductor laser facet reflectivities using free-space radiation modes”, *IEE Proc. Optoelectron*., vol. 140, no. 1, pp. 49-55, 1993.

[5] I. G. Tigelis, and A. B. Manenkov, “Scattering from an abruptly terminated asymmetrical slab waveguide”, *J. Opt. Soc. Amer*., vol. A-16, no. 3, pp. 523-532, 1999.

[6] I. G. Tigelis, and A. B. Manenkov, “Analysis of mode scattering from an abruptly ended dielectric slab waveguide by an accelerated iteration technique”, *J. Opt. Soc. Amer.*, vol. A-17, pp. 2249-2259, 2000.

[7] K. S. Yee, and J. S. Chen, “The finite-difference time-domain (FDTD) and the finite-volume time-domain (FVTD) methods in solving Maxwell's equations”, *IEEE Trans. Antennas Prop*., vol. 45, pp. 354-363, March 1997.

[8] S. T. Chu, and S. K. Chaudhuri, “A finite-difference time-domain method for the design and analysis of guided-wave optical structures”, *J. Lightwave Technol*., vol. 7, no. 12, pp. 2033-2038, 1989.

[9] J. Yamauchi, M. Mita, S. Aoki, and H. Nakano, “Analysis of antireflection coatings using the FD-TD method with the PML absorbing boundary condition”, *J. Lightwave Technol*., vol. 8, no. 2, pp. 239-241, 1996.

[10] J. R. Wait, “On the PML concept: a view from outside”, *IEEE Antennas Prop. Magazine*, vol. 38, no. 2, pp. 48-51, April 1996.

[11] R. Mittra, and U. Pekel, “A new look at the perfectly matched layer (PML) concept for the reflectionless absorption of electromagnetic waves”, *IEEE Microwave and Guided Wave Lett*., vol. 5, pp. 84-86, March 1995.

[12] J. P. Berenger, “Perfectly matched layer for the FDTD solution of wave-structure interaction problems”, *IEEE Trans. Antennas Prop*., vol. 44, pp. 110-117, Jan. 1996.

[13] A. B. Manenkov, “Irregular magneto-optical waveguides”, *IEEE Trans. Microwave Theory Tech.*, vol. MTT-29, no. 9, pp. 906-910, Sep. 1981.

[14] A. B. Manenkov “Eigenmodes expansion in lossy open waveguides (fibres)”, *Optical Quantum Electron.*, vol. 23, no. 5, pp. 621-632, 1991.

[15] D. Marcuse, *Theory of Dielectric Optical Waveguides*, London, Academic Press, 1991.

[16] M. J. Adams, *An Introduction to Optical Waveguides*, Chichester, John Wiley and Sons, 1981.